www.worldsciencepublisher.org

Radial Basis Function Neural Network based Approach to Estimate Transformer Harmonic Overvoltages

[*1,2]Iman Sadeghkhani, [3]Ali Yazdekhasti, [1]Arezoo Mortazavian, [4]Nima Haratian

[1]Department of Electrical Engineering, Islamic Azad University, Najafabad Branch, Najafabad, Iran
[2]Department of Electrical and Computer Engineering, Isfahan University of Technology, Isfahan, Iran
[3]Department of Electrical Engineering, University of Kashan, Kashan, Iran
[4]Department of Electrical Engineering, Allameh Feiz Kashani Institute of Higher Education, Kashan, Iran

Email: i.sadeghkhani@ec.iut.ac.ir, a-yazdekhasti@grad.kashanu.ac.ir, mortazavian@sel.iaun.ac.ir, haratian.nima@gmail.com

Abstract – This paper present an approach to evaluate overvoltages caused by transformer switching based on Radial Basis Function Neural Network (RBFNN). Such an overvoltage might damage some equipment and delay power system restoration. The developed ANN is trained with the worst case of the switching condition, and tested for typical cases. The simulated results for a partial of 39-bus New England test system, show that the proposed technique can estimate the peak values of switching overvoltages with good accuracy.

Keywords – Artificial neural networks; harmonic overvoltages; inrush current; power system restoration; radial basis function; transformer energization.

1. Introduction

During the early stages of restoring high voltage overhead and underground transmission lines, concerns are with three related overvoltages: sustained power frequency overvoltages, switching transients (surges), and harmonic resonance. In the early stages of the restoration, the lines are lightly loaded; resonance therefore is lightly damped, which in turn means the resulting resonance voltages may be very high [1], [2].

If the frequency characteristic of the system shows resonance conditions around multiples of the fundamental frequency, very high and weakly damped temporary overvoltages (TOVs) of long duration may occur when the system is excited by a harmonic disturbance, such as the switching of lightly loaded transformers or transformer saturation [2-4].

Overvoltage will put the transformer into saturation, causing core heating and copious harmonic current generation. Circuit breaker called upon to operate during periods of high voltage will have reduced interrupting capability. At some voltage even the ability to interrupt line-charging current will be lost [5-7].

In this paper power system blockset (PSB), a MATLAB/Simulink-based simulation tool [8], [9] is used for computation of temporary overvoltages. In order to study temporary overvoltages for a large number of possible system configurations, it is necessary to run many time-domain simulations resulting in a large amount of simulation time. A way to limit the overall calculation time is to reduce the number of simulations by applying analytical or knowledge-based rules to discard a number of system configurations before an actual time-domain simulation is carried out. This paper presents the ANN application for estimation of peak overvoltages under switching transients during transformer energization. A tool such as proposed in this paper that can give the maximum switching overvoltage will be helpful to the operator during system restoration. Also it can be used as training tool for the operators. In the proposed ANN we have considered the most important aspects, which influence the transient overvoltages such as source voltage, line length, switching angle, saturation curve slope and remanent flux. This information will help the operator to select the proper sequence of transformer to be energized safely with transients appearing safe within the limits. Results of the studies are presented for a partial of 39-bus New England test system to illustrate the proposed approach.

2. Overvoltages during Transformer Energization

This paper concentrates on the estimation of harmonic overvoltages. These are a result of network resonance frequencies close to multiples of the fundamental frequency. They can be excited by harmonic sources such as saturated transformers, power electronics, etc. They may lead to long lasting overvoltages resulting in arrester failures and system faults [1].

The major cause of harmonic resonance overvoltage problems is the switching of lightly loaded transformers at the end of transmission lines. The harmonic-current components of the same frequency as the system resonance frequencies are amplified in case of parallel resonance, thereby creating higher voltages at the transformer terminals. This leads to a higher level of saturation, resulting in higher harmonic components of the inrush current that again results in increased voltages This can happen particularly in lightly damped systems, common at the beginning of a restoration procedure when a path from a black-start source to a large power plant is being established and only a few loads are restored yet [2], [10].

Fig.1 shows the sample system considered for explanation of the proposed methodology which is a portion of 39-bus New England test system. Fig. 2 shows a sample switching overvoltages at bus 39 when transformer is energized.

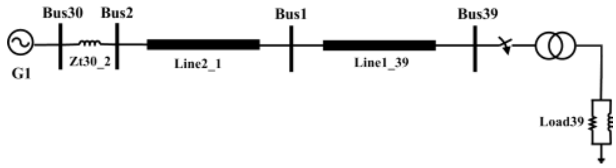

Figure 1. Power system at the beginning of a restoration procedure.

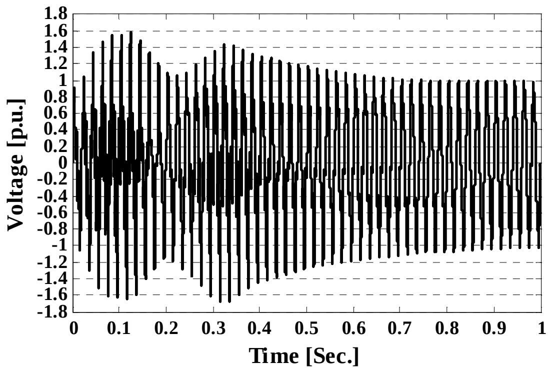

Figure 2. Voltage at bus 39 after switching of transformer for worst case condition.

In practical system a number of factors affect the overvoltages factors due to energization or reclosing. In this paper following parameters is considered:

- Source voltage
- Line length
- Closing time of the circuit breaker poles
- Saturation curve slope
- Remanent flux

Source voltage affects the overvoltage strongly. Fig. 3 shows the effect of source voltage on overvoltage peak at different remanent flux. Fig. 4 shows the effect of line length on overvoltages at different saturation curve slope. The saturation curve, and especially the L_{sat} i.e. the final slope of this curve, is a key point for the computation of the inrush currents but is not very easy to obtain. The transformer manufacturer provides a L_{sat} slope value with a dispersion usually considered of ±20 %. Fig. 5 shows effect of remanent flux on overvoltages at different line length. Fig. 6 shows the effect of saturation curve slope on overvoltages at different source voltage.

As discussed above for an existing system the main factors which affect the peak values of switching overvoltage are source voltage, line length, switching angle, saturation curve slope and remanent flux. Here it should be mentioned that a single parameter often cannot be regarded independently from the other important influencing factors. The magnitude of the overvoltages normally does not depend directly on any single isolated parameter and a variation of one parameter can often alter the influence of another parameter, in other words there exists an interaction between the various system and breaker parameters. This forbids the derivation of precise generalized rule of simple formulae applicable to all cases [11]. So an ANN can help to estimate the peak values of switching overvoltages generated during transformer energization. An ANN is programmed by presenting it with training set of input/output patterns from which it then learns the relationship between the inputs and outputs. In next section an ANN-based approach is described which can give a acceptable solution of switching transients by the help of which an operator can take a quick decision at the time of operation.

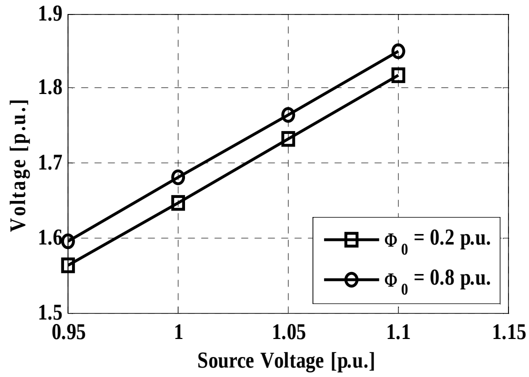

Figure 3. Overvoltage peak at bus 39 vs. source voltage: with line length = 100 km and saturation curve slope= 0.32 p.u.

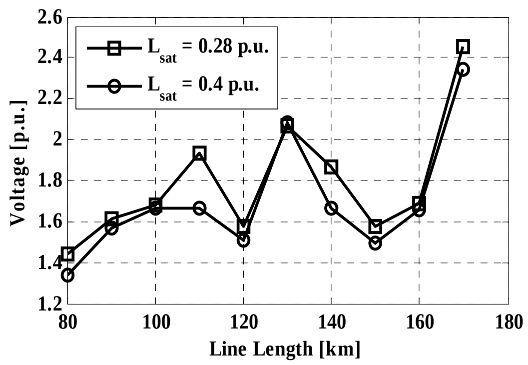

Figure 4. Overvoltage peak at bus 39 vs. line length: with source voltage=1 p.u. and remanent flux=0.8 p.u.

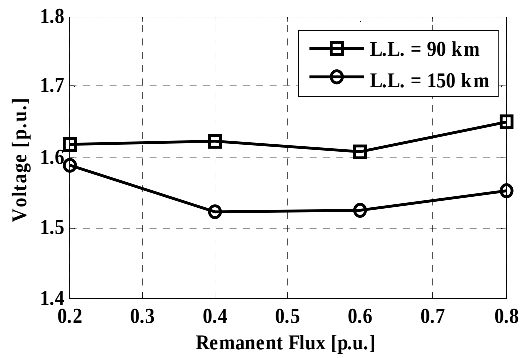

Figure 5. Overvoltage peak at bus 39 vs. remanent flux: with source voltage = 1 p.u. and saturation curve slope= 0.32 p.u.

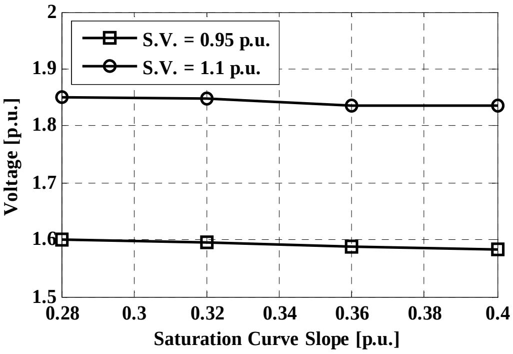

Figure 6. Overvoltage peak at bus 39 vs. saturation curve slope: with line length= 100 km and remanent flux= 0.8 p.u.

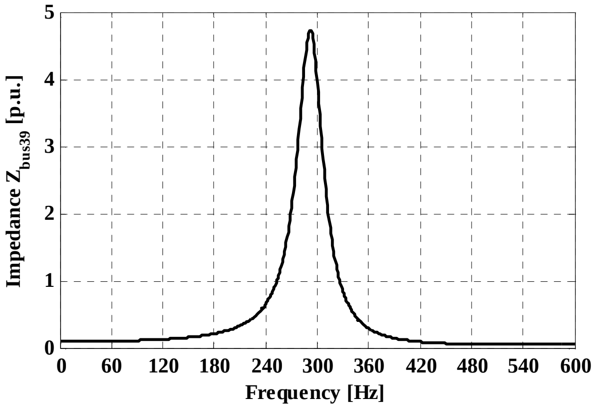

Figure 7. Impedance vs. frequency at bus 39.

3. Proposed Method for Harmonic Overvoltages Study

3.1. Worst Switching Condition Determination for Overvoltages Simulation

Normally for harmonic overvoltages analysis, the worst case of the switching condition must be considered which it is a function of switching time, transformer characteristics and its initial flux condition, and impedance characteristics of the switching bus [12]. Using the worst switching condition, the number of simulations for each case can be reduced significantly.

In order to determine worst-case switching time, the following index is defined as

$$W = \sum_{h=2}^{10} Z_{jj}(h) \cdot I_j(h, t_0, \phi_0) \tag{1}$$

where t_0 is the switching time and ϕ_0 is initial transformer flux. This index can be a definition for the worst-case switching condition. Using a numerical algorithm, one can find the switching time for which W is maximal (i.e., harmonic overvoltages is maximal).

Fig. 7 shows the result of the PSB frequency analysis at bus 39. The magnitude of the Thevenin impedance, seen from bus 39, Zbus39 shows a parallel resonance peak at 293 Hz. Fig. 8 shows changes of harmonic currents and *W* index with respect to the current starting angle [13], where *k* is harmonic number. Fig. 2 shows voltage at bus 39 after transformer switching for the worst-case condition (i.e., 17°) in one case. Table 1 summarizes the results of overvoltages simulation for three different switching conditions that verify the effectiveness of *W* index.

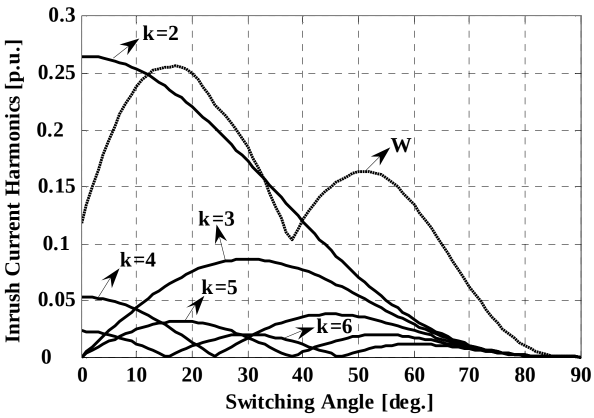

Figure 8. Changes of harmonic currents and W index vs. switching angle.

Table 1. Effect of switching time on the maximum of overvoltage and duration of $V_{peak} > 1.3$ p.u.

Switching Angle [deg.]	V_{peak} [p.u.]	Duration of ($V_{peak} > 1.3$ p.u.) [Sec.]
17	1.6791	0.3494
51	1.6318	0.2746
74	1.2847	0

3.2. Steps of Assessment and Estimation of Temporary Overvoltages

The steps for harmonic overvoltages assessment and estimation follow.

1) Determine the characteristics of transformer that must be energized.
2) Calculate the $Z_{ii}(h)$ at the transformer bus for h = $2f_0,\ldots,10f_0$.
3) Calculation of worst switching condition for simulation.
4) Run PSB simulation.
5) Calculation overvoltage peak.
6) Repetition of above steps with various system parameters to learning artificial neural network.
7) Testing artificial neural network with different system parameters.

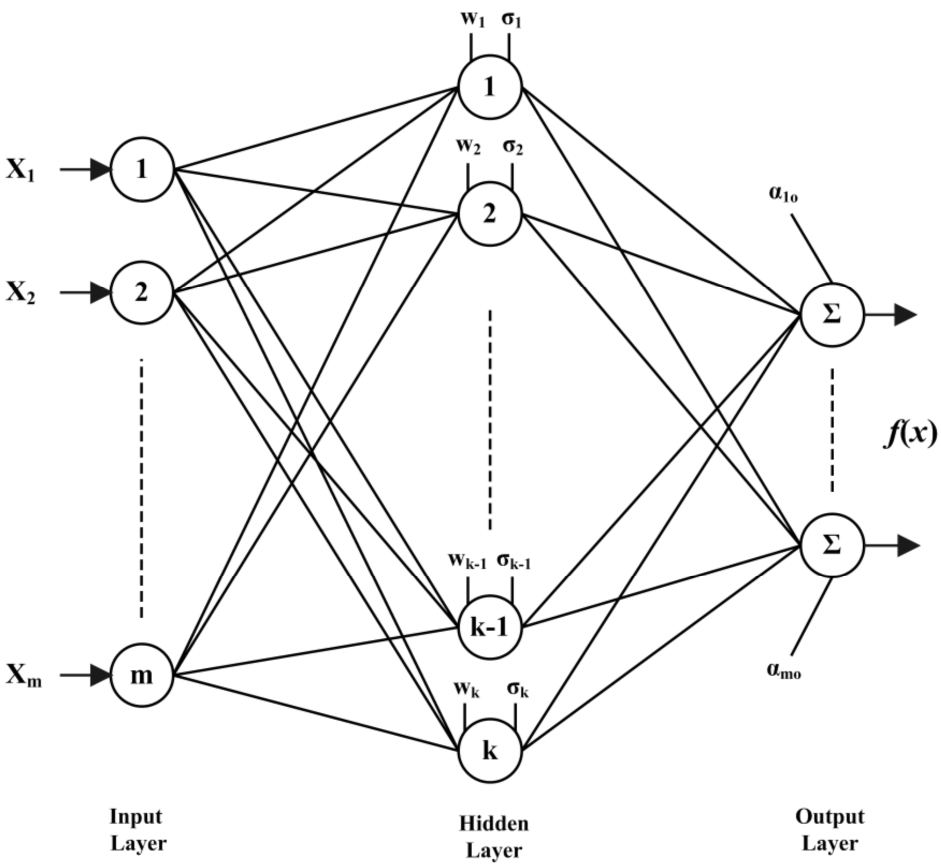

Figure 9. The structure of RBF neural network.

4. Radial Basis Function Neural Network

Fig. 9 shows the structure of the RBF neural network, which comprises of three layers. The hidden layer possesses an array of neurons, referred to as the computing units. The number of such units can be varied depending on user’s requirement [14], [15]. Different basis functions like spline, multiquadratic, and Gaussian functions have been studied, but the most widely used one is the Gaussian type. In comparison to the other types of neural network used for pattern classification like back propagation feedforward networks, the RBF network requires less computation time for learning and has a more compact topology. The Gaussian RBF is found not only suitable in generalizing a global mapping but also in refining local features without altering the already learned mapping. Each hidden unit in the network has two parameters called a center (ω) and a width (σ) associated with it. The response of one such hidden unit to the network input is expressed as

$$\phi_k(x_n) = \exp\left(-\frac{1}{\sigma_k^2}\|x_n - \omega_k\|^2\right) \qquad (2)$$

where ω_k is the center vector for kth hidden unit, σ_k is the width of the Gaussian function, and $\|\ \|$ denotes the Euclidean norm. The output layer comprises a number of nodes depending on the number of fault types to be classified which perform simple summation. The response of each hidden unit (1) is scaled by its connecting weights (α’s) to the output nodes and then summed to produce the overall network output. The overall network output is expressed as

$$f_m(x_n) = \alpha_{mo} + \sum_{k=1}^{N} \alpha_{mk}\phi_k(x_n) \qquad (3)$$

where k indicates the total number of hidden neurons in the network, α_{mk} is the connecting weight of the kth hidden unit to mth output node, and α_{mo} is the bias term for the corresponding mth output neuron.

The learning process of the RBFNN involves with the allocation of new hidden units and tuning of network parameters. The learning process is terminated when the output error goes under the defined threshold [16].

4.1. Testing

All experiments have been repeated for different system parameters. After learning, all parameters of the trained networks have been frozen and then used in the retrieval mode for testing the capabilities of the system on the data not used in learning. The testing data samples have been generated through the PSB program by placing the parameter values not used in learning, by applying different parameters. A large number of testing data have been used to check the proposed solution in the most objective way at practically all possible parameters variation. Percentage error is calculated as:

$$\text{error}(\%) = \frac{|\text{ANN} - \text{PSB}|}{\text{PSB}} \times 100 \qquad (4)$$

The proposed model tested with portion of 39-bus New England test system. Various cases of transformer energization are taken into account and corresponding peak values estimated from trained model.

Table 2. Case 1 some sample testing data and output

S.V.	L.L.	L_{sat}	Φ_0	V_{PSB}	V_{RBF}	$error_V$
0.925	95	0.34	0.1	1.4322	1.4061	1.8216
0.925	105	0.34	0.7	1.5868	1.5969	0.6392
0.925	135	0.38	0.5	2.0273	2.0523	1.2344
0.925	155	0.26	0.3	1.4626	1.4223	2.7549
0.975	85	0.34	0.3	1.3773	1.3509	1.9162
0.975	115	0.34	0.1	1.5817	1.5674	0.9025
0.975	145	0.3	0.7	1.7852	1.7703	0.8345
0.975	175	0.3	0.5	2.4214	2.3067	4.7359
1.025	105	0.38	0.3	1.7533	1.7884	2.0017
1.025	135	0.38	0.7	2.2154	2.2328	0.7842
1.025	155	0.34	0.1	1.5835	1.6044	1.3175
1.075	85	0.3	0.7	1.5817	1.5517	1.8936
1.075	95	0.26	0.7	1.7605	1.7025	3.2947
1.075	135	0.34	0.1	2.2708	2.2861	0.6742
1.075	175	0.38	0.1	2.8332	2.8954	2.1937

S.V. = source voltage, L.L. = line length [km], L_{sat} = saturation curve slope [p.u.], Φ_0 = remanent flux [p.u.], and $error_V$ = voltage error [%].

5. Case Study

In this section, the proposed algorithm is demonstrated for two case studies that are a portion of 39-bus New England test system, of which its parameters are listed in [17]. The simulations are undertaken on a single phase representation.

5.1. Case 1

Fig. 1 shows a one-line diagram of a portion of 39-bus New England test system which is in restorative state. The generator at bus 30 is a black-start unit. The load 39 shows cranking power of the later generator that must be restored by the transformer of bus 39. When the transformer is energized, harmonic overvoltages can be produced because the transformer is lightly loaded.

Results for a sample test data are presented in Table 2 and also shown in Figs. 10–11. Table 2 contains the some sample result of test data of case 1. Values in column V_{PSB} are the absolute values of peak voltage at bus 39 calculated by PSB program where the V_{RBF} values are the values simulated by trained network.

Fig. 10 shows overvoltage peak at bus 39 vs. the source voltage while other parameter like line length, saturation curve slope and remanent flux, constant at 125 km, 0.34 p.u. and 0.5 p.u., respectively. Fig. 11 shows overvoltage peak at bus 39 vs. the remanent flux when other parameter like source voltage, line length, saturation curve slope, constant at 1.025 p.u., 95 km and 0.26 p.u., respectively.

5.2. Case 2

As another example, the system in Fig. 12 is examined. It represents the same system as the one in Fig. 1, but a few restoration steps later. In the next step of the restoration, unit at bus 29 must be restarted. In order to provide cranking power for this unit, the transformer at bus 29 should be energized. In this condition, harmonic overvoltages can be produced because the load of the transformer is small.

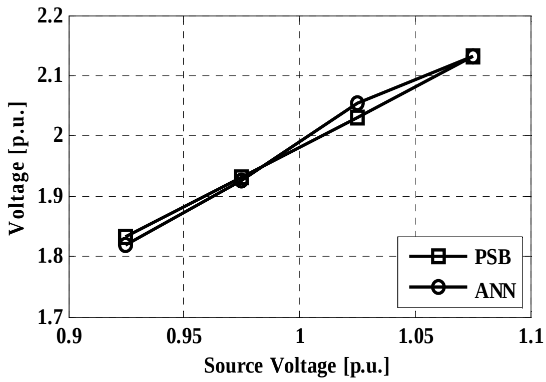

Figure 10. Overvoltage peak vs. source voltage at bus 39 simulated by ANN and PSB while line length 125^{km}, saturation curve slope 0.34$^{p.u}$. and remanent flux 0.5$^{p.u.}$.

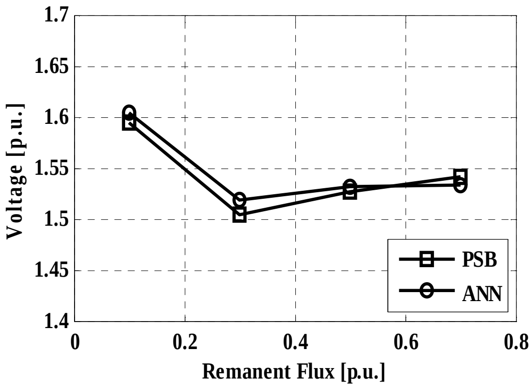

Figure 13. Overvoltage peak vs. remanent flux at bus 39 simulated by ANN and PSB while source voltage 1.025 p.u., line length 95 km and saturation curve slope 0.26 p.u..

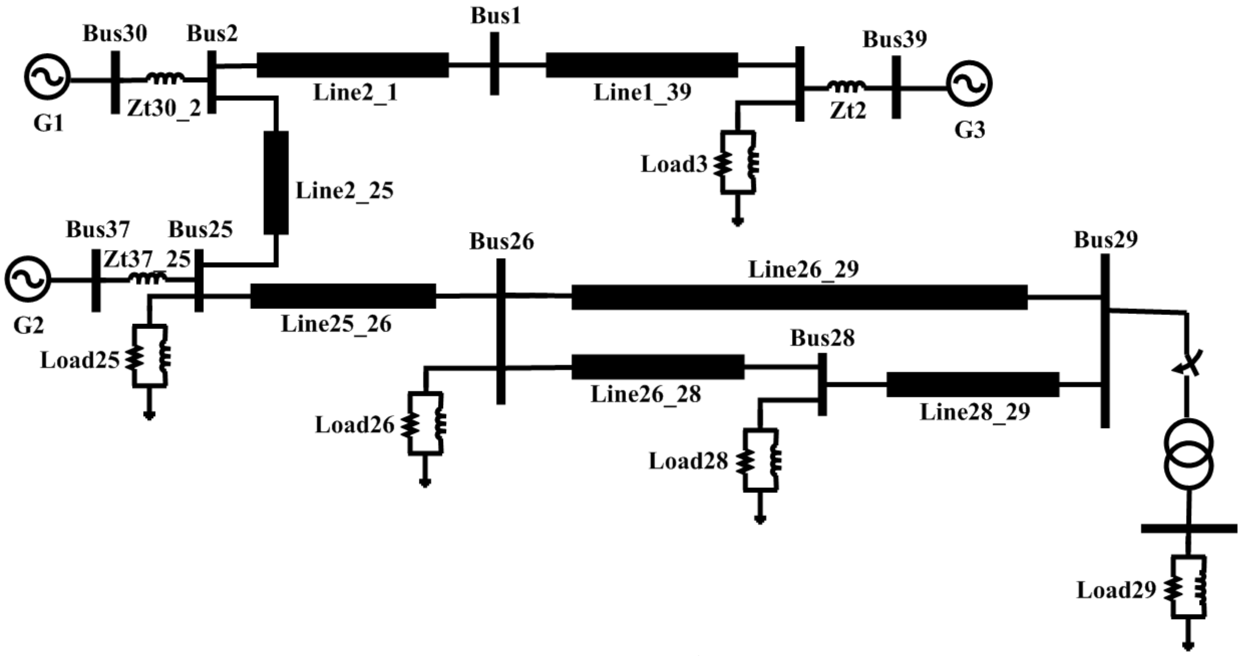

Figure 12. Studied system for case 2.

Table 3. Case 2 some sample testing data and output

S.V.	L.L.	L_{sat}	Φ_0	V_{PSB}	V_{RBF}	$error_V$
0.925	95	0.26	0.5	1.4995	1.5311	2.1074
0.925	115	0.34	0.3	1.6319	1.6527	1.2716
0.925	135	0.38	0.1	2.0581	2.1345	3.7109
0.925	165	0.3	0.7	1.8396	1.8121	1.4935
0.975	95	0.38	0.3	1.5387	1.5188	1.2948
0.975	125	0.34	0.3	1.9377	1.9082	1.5237
0.975	155	0.34	0.5	2.0493	2.0774	1.3694
0.975	175	0.26	0.7	2.0351	2.0177	0.8562
1.025	95	0.38	0.3	1.6183	1.6712	3.2706
1.025	125	0.34	0.3	2.0372	2.0445	0.3561
1.025	155	0.3	0.5	2.2047	2.1647	1.8126
1.075	95	0.26	0.5	1.7396	1.7915	2.9855
1.075	115	0.34	0.7	1.8967	1.8557	2.1629
1.075	145	0.38	0.5	2.3236	2.2807	1.8479
1.075	165	0.38	0.7	2.1047	2.0934	0.5376

S.V. = source voltage, L.L. = line length [km], L_{sat} = saturation curve slope [p.u.], Φ_0 = remanent flux [p.u.], and $error_V$ = voltage error [%].

The various cases of transformer energization are taken into account and corresponding peak overvoltages are computed from PSB program. Summary of few result are presented in Table 3. It can be seen from the results that the ANN is able to learn the pattern and give results to acceptable accuracy.

6. Conclusion

In this paper an RBFNN approach has been suggested to estimate the peak overvoltages due to transformer energization. The results from this scheme are close to results from the conventional method and helpful in predicting the overvoltage of the other case studies within the range of training set. The proposed ANN approach is tested on a partial 39-bus New England test system. This method omits time-consuming time-domain simulations and it is suitable for real time applications during system restoration. Also it can be used as a training tool for the operators.

7. References

[1] A. Ketabi, A.M. Ranjbar, and R. Feuillet, "Analysis and Control of Temporary Overvoltages for Automated Restoration Planning," IEEE Trans. Power Delivery, vol. 17 (2002), pp. 1121–1127.

[2] M.M. Adibi, R.W. Alexander, and B. Avramovic, "Overvoltage control during restoration," IEEE Trans. Power Syst., vol. 7 (1992), pp. 1464–1470.

[3] M.M. Adibi, J.N. Borkoski, and R.J. Kafka, "Analytical tool requirements for power system restoration," IEEE Trans. Power Syst., vol. 9 (1994), pp. 1582–1591.

[4] T. Hayashi et al., "Modeling and simulation of black start and restoration of an electric power system. Results of a questionnaire," Electra, no. 131 (1990), pp. 157–169.

[5] I. Sadeghkhani, "Using Artificial Neural Network for Estimation of Switching and Resonance Overvoltages during Bulk Power System Restoration," M.Sc. Thesis, Department of Electrical Engineering, University of Kashan (2009).

[6] I. Sadeghkhani, A. Ketabi, and R. Feuillet, "New Approach to Harmonic Overvoltages Reduction during Transformer Energization via Controlled Switching," in Proc. 15th International Conference on Intelligent System Applications to Power Systems, Curitiba, Brazil (2009).

[7] I. Sadeghkhani, A. Ketabi, and R. Feuillet, "Estimation of Temporary Overvoltages during Power System Restoration using Artificial Neural Network," in Proc. 15th International Conference on Intelligent System Applications to Power Systems, Curitiba, Brazil (2009).

[8] G. Sybille, P. Brunelle, L. Hoang, L. A. Dessaint, and K. Al-Haddad, "Theory and applications of power system blockset, a MATLAB/Simulink-based simulation tool for power systems," in Proc. IEEE Power Eng. Soc. Winter Meeting, pp. 774–779 (2000).

[9] A. Ketabi and I. Sadeghkhani, Electric Power Systems Simulation using MATLAB, Morsal Publications, Apr. 2011. (In Persian)

[10] G. Morin, "Service restoration following a major failure on the hydroquebec power system," IEEE Trans. Power Delivery, vol. 2 (1987), pp. 454–463.

[11] Cigre Working Group, "Switching overvoltages in EHV and UHV systems with special reference to closing and reclosing transmission lines," Electra 30 (1973), pp. 70–122.

[12] G. Sybille, M.M. Gavrilovic, J. Belanger, and V.Q. Do, "Transformer saturation effects on EHV system overvoltages," IEEE Trans. Power App. Syst., vol. PAS-104 (1985), pp. 671–680.

[13] O. Bourgault and G. Morin, "Analysis of harmonic overvoltage due to transformer saturation following load shedding on hydro-quebec-NYPA 765 kV interconnection," IEEE Trans. Power Delivery, vol. 5 (1990), pp. 397–405.

[14] S. Haykin, Neural Network: A Comprehensive Foundation, 2nd ed., Prentice Hall, 1998.

[15] M. Joorabian, S.M.A. Taleghani Asl, and R.K. Aggarwal, "Accurate fault locator for EHV transmission lines based on radial basis function neural networks," Electric Power Systems Research, vol. 71 (2004), p.p. 195–202.

[16] P.K. Dash, A.K. Pradhan, G. Panda, "Application of minimal radial basis function neural network to distance protection," IEEE Trans. Power Deliv., vol. 16, no. 1 (2001), pp. 68–74.

[17] S. Wunderlich, M. M. Adibi, R. Fischl, and C. O. D. Nwankpa, "An approach to standing phase angle reduction," IEEE Trans. Power Syst., vol. 9 (1994), pp. 470–478.

[18] Y. Zhang, L. Wu, "Rigid Image Registration by PSOSQP Algorithm", Advances in Digital Multimedia, vol. 1, no. 1 (2012), pp. 4-8

[19] A. Ahmadivand, "Enhanced and Optimal Current Limiter Based on Passive Magnetic Materials", Advances in Digital Multimedia, vol. 1, no. 1, (2012), pp. 19-28